Coupled Substitution of NiO and TiO_2 in Hematite

Bong-Hoon Park* and Dong-Su Kim

Division of Metals Examination, Korea Industrial Property Office, Taejon 302-173, Korea
Dept. of Environmental Sci. and Eng., Ewha Womans University, Seoul 120-750, Korea
Received October 1, 1998

The partitionings of NiO and of NiO and TiO_2 between hematite and Na_2O $2B_2O_3$ melts were studied by the flux growth method as a function of solute concentration. The substitution mechanisms of NiO and/or TiO_2 in -Fe_2O_3 lattice were discussed based on the concentration dependence of the distribution coefficients. The substitution of Ni^{2+} ion for Fe^{3+} was accompanied by the charge compensating oxygen ion vacancies, while the coupled substitution of Ni^{2+} and Ti^{4+} ions for Fe^{3+} was accompanied by the formation of Fe^{2+} ion, which was confirmed by chemical analysis.

Introduction

It is well known that impurities and size distribution of α-Fe_2O_3, main raw material for the ferrite products, show significant effects on their magnetic properties. Therefore, thermodynamic studies on trace (or minor) elements in α-Fe_2O_3 are indispensable in clarifying the impurity behavior. A series of experiments on the distribution coefficients of TiO_2 between α-Fe_2O_3 crystals and Na_2O-B_2O_3 flux were reported by Suito and coworkers.[1,2] The studies for manganese and Al_2O_3 partitions also have been reported.[2] With this background in mind, we are interested in elucidating the mechanism of NiO and/or TiO_2 distribution in α-Fe_2O_3. For the measurement of the distribution coefficients of NiO and/or TiO_2 between α-Fe_2O_3 crystal and $Na_2O \cdot 2B_2O_3$ flux, the method of crystal growth by Ostwald ripening was used in the present work. Here we report on the mechanism of the coupled substitution of NiO and TiO_2 in α-Fe_2O_3 lattice.

Experimental

Method. α-Fe_2O_3 (> 99.99 wt.%) was purchased from Rare Metallic Co. and $Na_2B_4O_7$, NiO, and TiO_2 were all reagent grade (Aldrich Co.). The average size of α-Fe_2O_3 crystals determined by scanning electron microscope (SEM) was 0.1 m. A little excess of α-Fe_2O_3 powder, about 1.5 times greater than the solubility,[1] was mixed with the $Na_2O \cdot 2B_2O_3$ flux. Samples (20-30 g) in a Pt crucible were placed in the constant temperature zone of a vertical SiC resistance furnace and stirred with a Pt stirrer (10 rad/sec) to make the liquid composition homogeneous. The experiments were conducted under a dry air atmosphere at temperature ranging from 900 to 1100 °C in the experiments of NiO partitioning and at 1000 °C in the coupled substitution of NiO and TiO_2. In most experiments, a solute sample in α-Fe_2O_3 crystals was obtained from the solution side.

After standing at room temperature for 6-12 hr, the sample was quenched in water. No α-Fe_2O_3 crystal was precipitated on quenching. The contents of each element in the solid and liquid phases of the sample were measured by wet chemical analysis. All the water used in the experiment was prepared by distillation and deionization and its resistance was at least 18 MΩ. More detailed descriptions are described in the previous reports.[1,2]

Analysis. The sample (1 g) was washed in boiling HCl (2 50) solution (100 mL) for 30 min to dissolve the flux. Thereafter, the aqueous solution was separated from the crystals by pressurized filtration, using a 0.1 μm membrane filter. H_2SO_4 (1+35) was used with samples containing TiO_2. The flux compositions were determined by analyzing the filtrate. α-Fe_2O_3 crystals (0.2 g) were dissolved in 10 mL of hot HCl (1 1) solution.

The Fe^{2+} ion content in α-Fe_2O_3 crystals was determined by potassium dichromate titration after dissolving crystals with HCl (1+1) under dry CO_2 atmosphere. Atomic absorption spectrometry was used for the analysis of Na, and inductively coupled plasma (ICP) emission spectrometry (SEIKO, SPS-1200A) for the analysis of the other elements.

The contents of each element in both the α-Fe_2O_3 crystal and the flux was analyzed by electron probe micro-analysis (EPMA; Hidachi, X650S) at an accelerating voltage of 15 kV for all elements. The results were in good agreement with those obtained by chemical analysis. Homogeneity of Ni and Ti in crystal grains was confirmed by line analysis of EPMA.

Results and Discussion

Crystal growth by Ostwald ripening. The initial α-Fe_2O_3 crystals with an average size of 0.1 μm in a saturated solution were found to grow to the size of 10-20 μm in a period of 6-12 hr. The observed coarsening of crystals was attributable to the Ostwald ripening mechanism in which the driving force is the reduction of total interfacial energy of the larger crystals. The details of this mechanism are discussed elsewhere.[1]

The partitioning of minor elements occurs under equilibrium conditions during Ostwald ripening, due to the low degree of supersaturation with respect to crystal growth. This was confirmed by examining the homogeneity and time dependence of the solute content in crystal grain. The concentration of a solute within a crystal was homogeneous and constant with time in the present work. In the previous works[1,2] the equilibrium partitioning was confirmed by examining the effect of initial grain size on the distribution coefficient and the reverse experiment, in which a solute element was dissolved from crystal into flux, was carried out. These previous experimental findings lead to the conclusion that the equilibrium distribution coefficients can be obtained using the flux growth method. The contents of Na_2O and B_2O_3 in α-Fe_2O_3 were analyzed to be 10-25 and 10-30 wt. ppm, respectively.

Substitution of NiO by defect formation. The distribution coefficient of NiO between solid and liquid phases is defined as follows:

$$k_{NiO}\ x^{s}_{NiO} / x^{l}_{NiO} \qquad (1)$$

where x^{s}_{NiO} and x^{l}_{NiO} represent the mole percent of NiO in solid and liquid phases, respectively.

The relationships between the distribution coefficient of NiO and the content of NiO in the $Na_2O{\cdot}2B_2O_3$ flux expressed by mole percent, are plotted as a function of temperature in Figure 1. It is shown that the distribution coefficient of NiO decreases with increase of the content of NiO in flux.

When a different valence ion enters the substitutional site at compositions of greater than thermal defect concentration, lattice defects are produced due to charge neutrality. This leads to the decrease of a distribution coefficient.[3,4,5] Although the distribution coefficient also depends on a solution interaction factor, it seems to be quite sensitive to changes in solid phase in the present experimental conditions.

Incorporation of NiO into α-Fe_2O_3 by the substitution of Ni^{2+} ion for Fe^{3+} sites leads to charge compensating oxygen ion vacancies according to the following equation:

Using the Kröger and Vink notation,[6] we obtain

$$NiO(l) = Ni'_{Fe} + O^{x}_{O} + (1/2)V''_{O} \qquad (2)$$

The equilibrium constant, K_2, for the reaction given by Eq. (2) can be expressed by

$$K_2 = [Ni'_{Fe}][V''_{O}]^{1/2} f(\gamma) / x^{l}_{NiO} \qquad (3)$$

where [i] and x_i denote the molar concentration of i component and $f(\gamma)$ is the respective activity coefficient term. The activity of O^{x}_{O} remains essentially constant and can be taken as a unit.

Salmon[7] has reported that Fe_2O_3 is oxygen deficient and for Fe_2O_3 in equilibrium with Fe_3O_4, the value of x in $Fe_2O_{3\ x}$ ranges from 0.0015 at 1000 °C to 0.011 at 1450 °C. Thus, if we assume that the concentration of thermal oxygen vacancy is negligible, we can write

$$[V''_{O}] = (1/2)[Ni'_{Fe}] \qquad (4)$$

By substituting Eq. (4) into Eq. (3) and expressing $[Ni'_{Fe}]$ by x^{s}_{NiO}, we have

$$x^{s}_{NiO} = C_1\{K_2/f(\gamma)\}^{2/3}(x^{l}_{NiO})^{2/3} \qquad (5)$$

where C_1 is the constant under the present experimental conditions. If a dilute solution behavior (Henry's law) is valid with respect to NiO in both phases, it can be expected that x^{s}_{NiO} is proportional to x^{l}_{NiO} to the power of 2/3. This relationship is shown in Figure 2, demonstrating a good linearity at temperatures examined.

The importance of thermal defects in the very low concentration region has been confirmed experimentally by Harrison and Wood[8] who studied the partitioning of Sm and Tm between garnets and melts. They found that the distribution coefficient becomes constant at very low concentrations of rare earth metals. Wagner[9] also discussed the decisive role of lattice defects on the distribution of $SrCl_2$ between solid and liquid KCl.

Coupled substitution of NiO and TiO_2. The charge compensating substitutions are termed coupled diadochy[10] or compensatory solid solution.[11] "Coupled substitution" is designated by Nassau[4] who studied the distribution of various rare earths in the Czochralski growth of calcium tungstate crystals from melt. In this study, the designation "coupled

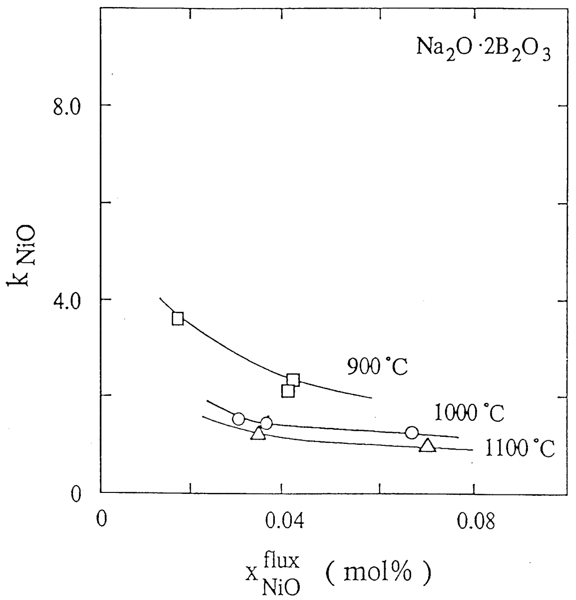

Figure 1. Distribution coefficient of NiO plotted against NiO content in flux as a function of temperature.

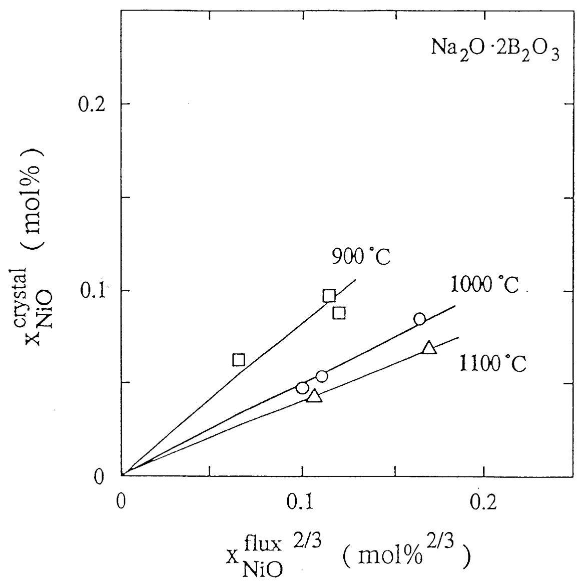

Figure 2. NiO content in crystal plotted against the two-thirds power of NiO content in flux.

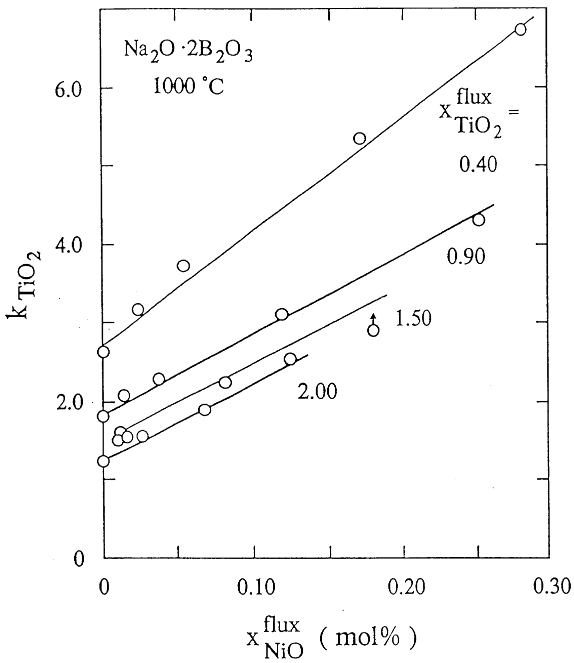

Figure 3. Effect of NiO content in flux on k_{TiO2} as a function of TiO_2 content in flux.

substitution" is used. The coupled substitution of NiO and TiO_2 in -Fe_2O_3 is discussed in this section based on results obtained in the NiO and TiO_2 partitioning experiments.

The values for k_{TiO2} are plotted against the NiO content in flux, as a function of TiO_2 content in flux in Figure 3, in which the results at x^{flux}_{NiO} 0 correspond to those obtained at 1000 °C in the previous experiment[2] of TiO_2 partitioning. It is shown that k_{TiO2} increases with increase of NiO content in flux at constant TiO_2 content in flux.

In order to explain the mechanism for coupled substitution, the content of Fe^{2+} ion in α-Fe_2O_3 was determined by chemical analysis. The sum of the FeO and NiO contents in α-Fe_2O_3 is plotted against the TiO_2 content in crystal in Figure 4, in which a reasonable linearity was obtained. This implies that 2 mol of Fe^{3+} ion is substituted with x mol of Ni^{2+} ion, (1-x) mol of Fe^{2+} ion, and 1 mol of Ti^{4+} ion.

The values for k_{NiO} are plotted against the TiO_2 content in flux as a function of NiO content in flux in Figure 5. The result at x^{flux}_{TiO2} 0 corresponds to that obtained at 1000 °C in NiO partitioning experiments mentioned above. This marked increase of k_{NiO} indicates that the coupled substitution, not accompanied by formation of lattice defect in α-Fe_2O_3 via the charge-balanced mechanism, requires less energy than the substitution accompanied by oxygen ion vacancy formation. As is the result for k_{TiO2} shown in Figure 3, k_{NiO} increases with increase of TiO_2 content in flux at constant NiO content in flux. It can be demonstrated that the increment of k_{NiO} is greater than that of k_{TiO2}. The reason for this may be explained as follows. The substitution accompanied by oxygen ion vacancy according to Eq. (2) occurs in the experiment of NiO partitioning in α-Fe_2O_3. On the other hand, the substitution accompanied by the Fe^{2+} formation according to Eq. (6) occurs in the experiment of TiO_2 partitioning in α-Fe_2O_3.[3] Thus, the increment of k_{NiO} is greater than those for k_{TiO2}, since the latter requires less energy than the former.

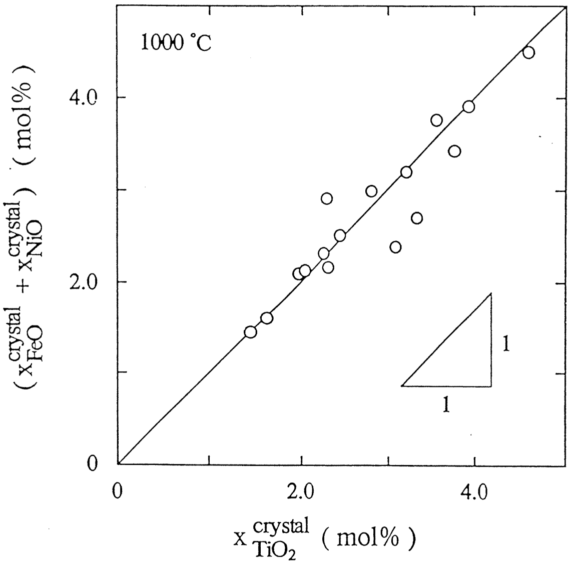

Figure 4. Relationship between the sum of FeO and NiO contents and TiO_2 content in crystal.

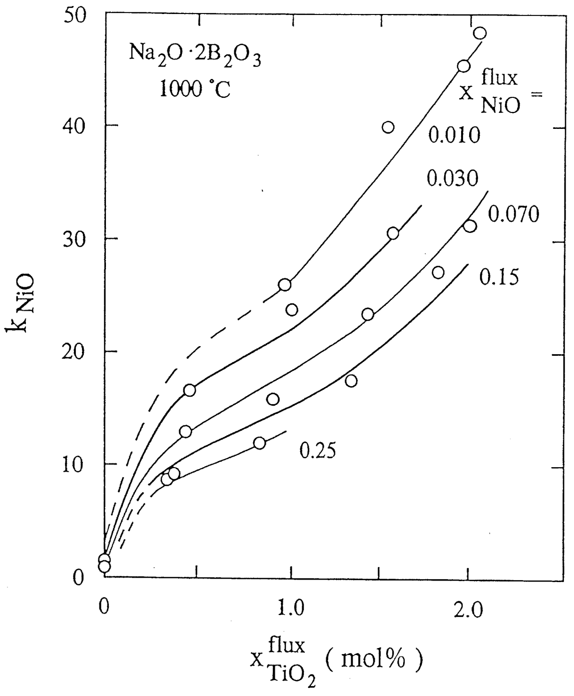

Figure 5. Effect of TiO_2 content in flux on k_{NiO} as a function of NiO content in flux.

$$TiO_2(l) + Fe^{x}_{Fe} = Ti_{Fe} + Fe'_{Fe} + 2O^{x}_{O} \qquad (6)$$

where the symbol Fe_{Fe} refers to the Fe^{2+} ion.

Roy and Coble[12] studied the coupled substitution of MgO and TiO_2 in Al_2O_3 and proposed the defect equilibrium: $MgTiO_3(s) = Mg'_{Al} + Ti_{Al} + 3O^{x}_{O}$ in which the electroneutrality is maintained. In the present study, the coupled substitution of TiO_2 and NiO in α-Fe_2O_3 can be written as

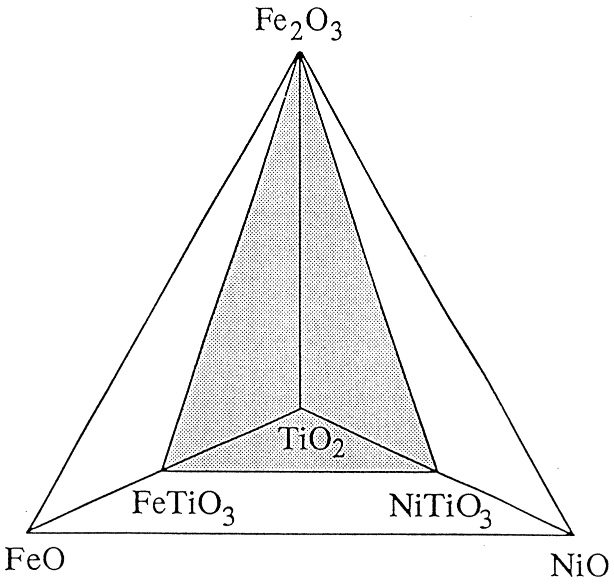

Figure 6. Solid solution surface of Fe_2O_3 and $Ni_{1-x}Fe_xTiO_3$ rhombohedral phases in the NiO-FeO-Fe_2O_3-TiO_2 tetrahedron.

$$NiO(l) + TiO_2(l) = Ni'_{Fe} + Ti_{Fe} + 3O^x_O \tag{7}$$

In the Fe_2O_3-FeO-TiO_2-NiO tetrahedron shown in Figure 6, the substitution given by Eq. (7) corresponds to the solid solution of $NiTiO_3$ in α-Fe_2O_3 in the Fe_2O_3-$NiTiO_3$ pseudo binary system. However, as mentioned previously, the formation of Fe^{2+} ion was experimentally confirmed as a result of coupled substitution. Therefore, it appears reasonable that the substitution according to Eq. (8) which is the combination of Eq.'s (6) and (7), becomes energetically more favorable.

$$NiO(l) + 2TiO_2(l) + Fe^x_{Fe} = Ni'_{Fe} + 2Ti_{Fe} + Fe'_{Fe} + 5O^x_O \tag{8}$$

The reaction given by Eq. (8) corresponds to the solid solution of $FeTiO_3$ and $NiTiO_3$ in α-Fe_2O_3- the Fe_2O_3-$FeTiO_3$-$NiTiO_3$ pseudo ternary system shown in Figure 6, which is predicted from the Fe_2O_3-$FeTiO_3$-$MgTiO_3$ pseudo ternary system.[13]

From Eq. (8), we obtain

$$\log(x^s_{FeO}) = -\log(k_{NiO}\cdot k^2_{TiO2}) + C_2 \tag{9}$$

where C_2 is the constant in the present work.

The values for x^s_{FeO} are plotted against the term $k_{NiO}\cdot k^2_{TiO2}$ on logarithmic scales in Figure 7, indicating a linearity having a slope of -1. This suggests that Henry's law is approximately valid in each component in both phases.

Conclusions

Distribution experiments of NiO and/or TiO_2 between α-Fe_2O_3 crystal and $Na_2O\cdot 2B_2O_3$ melt were carried out. With respect to the substitution mechanism in α-Fe_2O_3, we reached the following conclusions from the composition dependence of the distribution coefficient.

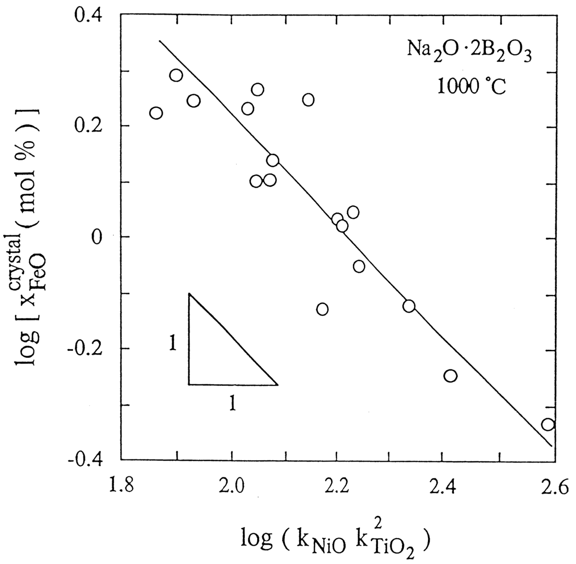

Figure 7. FeO content in crystal plotted against $k_{NiO}\ k^2_{TiO2}$ term in Eq. (9) on logarithmic scales.

i) NiO, on dissolving in α-Fe_2O_3, produces oxygen ion vacancies.

ii) The coupled substitution of NiO and TiO_2 in α-Fe_2O_3 accompanied by the formation of Fe^{2+} ions was explained by the solid solution of the rhombohedral $Ni_xFe_{(1-x)}TiO_3$ and α-Fe_2O_3 phases.

References

1. 1. Park, B.; Suito, H. *ISIJ Int.* **1990**, *30*, 426.
2. 2. Todoroki, H.; Suito, H. *Scand. J. Metall.* **1991**, *20*, 211.
3. 3. Kelting, H.; Witt, H. *Z. Phys.* **1949**, *126*, 697.
4. 4. Nassau, K. *J. Phys. Chem. Solids* **1963**, *24*, 154.
5. 5. Shannon, R. D. *Acta Cryst.* **1976**, *A32*, 752.
6. 6. Kröger, F. A. In *Solid State Physics*; Seitz, F.; Turnbull, D., Eds.; Academic Press: New York, **1956**; p 307.
7. 7. Salmon, O. N. *J. Phys. Chem.* **1961**, *65*, 550.
8. 8. Harrison, W. J.; Wood, B. J. *Contrib. Mineral. Petrol.* **1980**, *72*, 145.
9. 9. Wagner, C. *Phys. Chem.* **1953**, *57*, 738.
10. 10. Eite, W. *The Physical Chemistry of the Silicates*, 3rd Ed.; University of Chicago Press: **1954**; p 75.
11. 11. Smith, F. G. *Physical Geochemistry*; Addison-Wesley: **1963**; p 42.
12. 12. Roy, S. K.; Coble, R. L. *J. Am. Ceram. Soc.* **1968**, *51*, 1.
13. 13. Speidel, D. H. *Am. J. Sci.* **1970**, *268*, 341.